Atmosphere **2015**, *6*, 1590-1607; doi:10.3390/atmos6111590

OPEN ACCESS

atmosphere

ISSN 2073-4433

www.mdpi.com/journal/atmosphere

Article

CCN Properties of Organic Aerosol Collected Below and within Marine Stratocumulus Clouds near Monterey, California

Akua Asa-Awuku [1,2,*], Armin Sorooshian [3], Richard C. Flagan [4], John H. Seinfeld [5] and Athanasios Nenes [5,6,7]

1 Department of Chemical and Environmental Engineering, University of California, Riverside, Riverside, CA 92521, USA

2 Bourns College of Engineering, Center for Environmental Research and Technology, University of California, Riverside, Riverside, CA 92507, USA

3 Departments of Chemical and Environmental Engineering, and Atmospheric Sciences University of Arizona, Tucson, AZ 85721, USA; E-Mail: armin@email.arizona.edu

4 Department of Chemical Engineering, California Institute of Technology, Pasadena, CA 91125, USA; E-Mail: flagan@cheme.caltech.edu

5 Schools of Chemical and Biomolecular Engineering and Earth and Atmospheric Sciences, Georgia Institute of Technology, Atlanta, GA 30332, USA; E-Mail: seinfeld@caltech.edu

6 Institute of Chemical Engineering Sciences, FORTH, Patras, GR-26504, Greece

7 Institute of Environmental Research and Sustainable Development, National Observatory of Athens, Palea Penteli, GR-15236, Greece

* Author to whom correspondence should be addressed; E-Mail: akua@engr.ucr.edu; Tel.: +1-951-781-5785; Fax: +1-951-781-5790.

Academic Editor: Robert W. Talbot

Received: 31 August 2015 / Accepted: 10 October 2015 / Published: 28 October 2015

Abstract: The composition of aerosol from cloud droplets differs from that below cloud. Its implications for the Cloud Condensation Nuclei (CCN) activity are the focus of this study. Water-soluble organic matter from below cloud, and cloud droplet residuals off the coast of Monterey, California were collected; offline chemical composition, CCN activity and surface tension measurements coupled with Köhler Theory Analysis are used to infer the molar volume and surfactant characteristics of organics in both samples. Based on the surface tension depression of the samples, it is unlikely that the aerosol contains strong surfactants. The activation kinetics for all samples examined are consistent with rapid $(NH_4)_2SO_4$ calibration aerosol. This is consistent with our current understanding of droplet kinetics for ambient CCN. However, the carbonaceous material in cloud drop residuals is

far more hygroscopic than in sub-cloud aerosol, suggestive of the impact of cloud chemistry on the hygroscopic properties of organic matter.

Keywords: marine aerosol; organics; stratocumulus clouds; cloud condensation nuclei

1. Introduction

It is well established that organic compounds (especially water-soluble organic compounds, WSOC) are ubiquitous in marine aerosol; they can interact with water and affect aerosol hygroscopicity, droplet surface tension, and Cloud Condensation Nuclei (CCN) activity [1–6]. As a result, marine aerosol organic matter can affect cloud droplet number concentration as much as 15% [7–10] and may exert a climatically important impact on clouds.

Organic compounds, depending on their source, are classified as "primary" and "secondary". Primary organic marine aerosol (POMA) can include high molecular-weight compounds transferred onto sea-salt aerosol from the surfactant-rich surface ocean during the bubble-bursting process [9]. The presence of POMA is mostly attributed to biological activity, and its concentration varies with season [9,11,12]. POMA can exhibit low hygroscopic growth factors but maintain high CCN activity [13] or *vice versa* [14]. Secondary organic marine aerosol (SOMA) can be produced during cloud processing [15–19]; perhaps the most studied chemical pathway for SOMA is glyoxylic acid oxidation [20] via several aqueous phase intermediates [21–23]. Continental biogenic emissions can also contribute to organic mass in marine clouds at high altitudes [24]. Anthropogenic emissions can substantially contribute to marine organics; for example, particulate emissions from ships are composed roughly of up to 10% carbon [25,26], in the form of sparingly soluble poly-aromatic hydrocarbons, ketones and quinones (PAHs, PAKs, and PAQs, respectively [13,27]). "Ship tracks" are a natural laboratory for studying aerosol indirect effects, as clouds with uniform dynamics, are exposed to a strong gradient in emissions concentrations and often exhibit droplet number, effective radius and drizzle rates responses that are consistent with local emission rates [28–32].

In this study, marine aerosol samples influenced by ship emissions are collected in-situ (in and out of cloudy regions) and studied for their cloud-droplet formation properties. Given the complexity of the water-soluble organic fraction, characterization is done by measuring the size-resolved CCN activity of the material, surface tension depression and using Köhler Theory Analysis (KTA) [33–35] to infer the thermodynamic properties (average molar volume, surfactant tension depression) of the organic fraction and its potential impact on droplet growth rate kinetics. These properties are then related to the influence of primary emissions and in-cloud oxidation processes on the CCN activity of the organic compounds.

2. Experimental Methods

2.1. Aerosol Sampling and Chemical Composition

The samples analyzed in this study were obtained during the Marine Stratus/Stratocumulus Experiments (MASE) that took place near the coast of Monterey, California, from July to August

2005. The airborne platform used the Center for Interdisciplinary Remotely-Piloted Aircraft Studies (CIRPAS) Twin Otter that sampled boundary layer air over 13 flights. A full description of the aerosol and cloud instrument payload aboard the plane during the MASE campaign can be found in Lu *et al.* [36]. Six of thirteen flights encountered strong, localized perturbations in aerosol concentration, size, and composition consistent with ship emissions. The data presented here were sampled on 13 July in the vicinity of ship tracks. An overview of airborne studies conducted in this region has been summarized by Coggon *et al.* [18].

Two sample types were collected aboard the aircraft in this study: cloud droplet residuals (CR) from evaporated cloud droplets, and sub-cloud (SC) aerosol sampled below cloud (and occasionally in clear-sky conditions). CR samples were collected with a counter-flow virtual impactor (CVI) [37,38], in which cloud droplets with diameter greater than 5 μm were inertially separated from interstitial (unactivated) aerosol and evaporated before collection. Analysis of cloud droplet residuals with this approach has been instrumental in understanding the origin of CCN in ambient clouds [18].

Table 1. Concentrations of Water Soluble Organic Carbon (WSOC) and ions ($mg \cdot L^{-1}$ sample), and, α ($mN \cdot m^{-1} \cdot K^{-1}$) and β ($L \cdot mg^{-1}$) parameters of the Szyszkowski–Langmuir surface tension model * [45] fits for the aerosol samples analyzed.

Property	Cloud Residuals (CR)	Sub-Cloud (SC)
WSOC	220 ± 14	202 ± 7
Ca^{2+}	3.10	2.75
Mg^{2+}	0.07	0.58
Na^{+}	21.07	20.90
Cl^{-}	25.30	22.61
NH_4^{+}	21.00	36.38
NO_3^{-}	16.12	17.30
SO_4^{2-}	35.30	87.85
Oxalate	3.61	4.22
α	8.99×10^{-4}	2.91×10^{-3}
β	3.84×10^{-2}	1.63×10^{-2}

* Szyszkowski–Langmuir Equation (1): $\sigma = \sigma_w - \alpha T \ln(1 + \beta c)$.

A Brechtel Manufacturing Inc. Particle-Into-Liquid sampler (PILS; [20]) was used to collect the water-soluble fraction of SC and CR by exposing the aerosol to supersaturated steam and growing them into droplets that are subsequently collected by inertial impaction. The liquid stream was then collected in vials over 3.5 to 5 min each. The chemical composition of the ionic species in each sample was measured with a dual Ion Chromatography (IC) system (ICS-2000 with 25 μL sample loop, Dionex Inc.); the IC detection limit of aerosol species is less than 0.1 $\mu g \cdot m^{-3}$ for inorganic ions (Na^{+}, NH_4^{+}, K^{+}, Mg^{2+}, Ca^{2+}, Cl^{-}, NO_3^{-}, NO_2^{-}, and SO_4^{2-}) and less than 0.01 $\mu g \cdot m^{-3}$ air for the organic acid ions (dicarboxylic acids C_2–C_9, acetic, formic, pyruvic, glyoxylic, maleic, malic, methacrylic, benzoic, and methanesulfonic acids). The WSOC content was also measured off-line with a Total Organic Carbon (TOC) Analyzer (Sievers Model 800 Turbo, Boulder, CO) (Table 1). The contents of the vials were subsequently analyzed for their CCN activity and surfactant characteristics (Sections 2.2–2.4). The aerosol samples analyzed in the study were obtained on 13 July (when the highest organic acid concentrations were reported) from within and below cloud (cloud base and cloud top were measured

at 101 and 450 m altitude, respectively) [36]. During this flight, the aircraft focused on sampling air in the vicinity of ship tracks. Backward trajectories calculated using the NOAA HYSPLIT (HYbrid Single-Particle Lagrangian Integrated Trajectory) model (http://www.arl.noaa.gov/ready/hysplit4.html) indicate that the air mass on the 13 July originated from the North Pacific; the vertical profile indicates that the aerosol masses sampled on 13 July originated from the free troposphere before descending into the marine boundary layer (Figure 1).

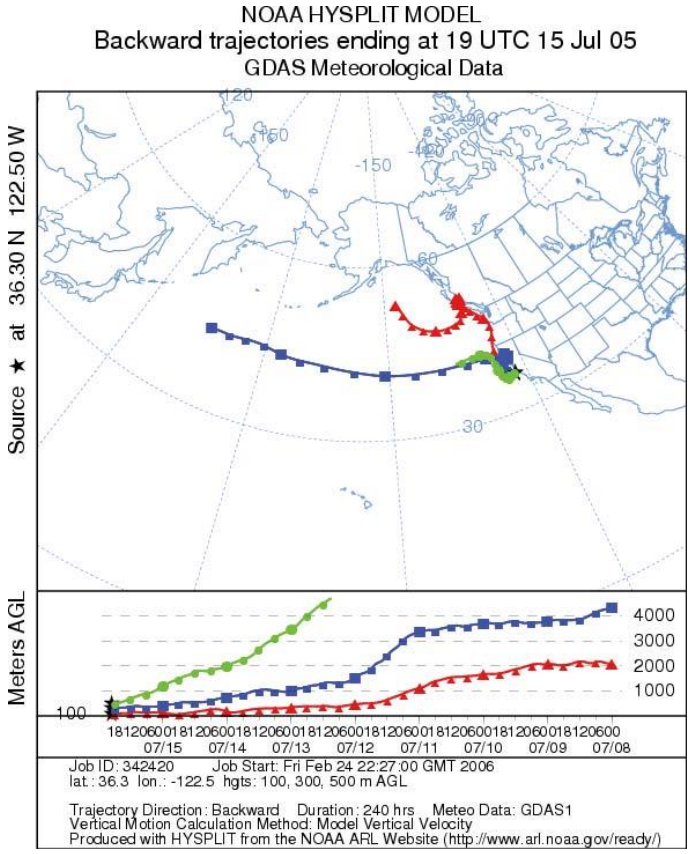

Figure 1. NOAA HYSPLIT (HYbrid Single-Particle Lagrangian Integrated Trajectory) Model Back Trajectories for air masses sampled aboard the Twin Otter on 13 July 2005.

2.2. CCN Activity of Soluble Material Collected

The aqueous contents of the PILS vials were atomized with a Collison-type atomizer (Figure 2) operated at 5 psig pressure. The atomized aerosol was then dried through two silica gel diffusional dryers, charged by a Kr-85 bipolar charger, and classified with a Differential Mobility Analyzer (DMA 3081) (Figure 2). The classified monodisperse aerosol was then split and passed through a TSI 3025A Condensation Particle Counter (CPC) to measure aerosol number concentration (CN); the other stream was sampled by a Droplet Measurement Technologies Continuous-Flow Streamwise Thermal Gradient CCN Counter (CFSTGC) [39–41]. Given the limited amount of sample, size-resolved CCN activity and growth kinetics measurements were obtained using scanning mobility CCN Analysis (SMCA) [42]. The SMCA process couples CFSTGC measurements with a scanning mobility particle sizer (SMPS). An inversion procedure was used to compute the ratio of CCN to CN as a function of aerosol size as the SMPS scans from 10 and 250 nm dry mobility diameter for a fixed supersaturation, *s*. The data were fit to a sigmoidal function, corrected for diffusion and multiple charges in the

DMA [42]; the particle dry diameter size, d, for which 50% of the particles activated into droplets, represents the dry diameter of the particle with critical supersaturation, s_c, equal to the instrument supersaturation. The activation experiments were repeated (a minimum of four times) for each s level, which varied from 0.2% to 1.2%. The compositional data, aerosol surfactant behavior, and the dependence of d with respect to s_c, were used to infer the molar volume and surfactant characteristics of the organic fraction with Köhler Theory Analysis [33–35,43] (Section 3). The CFSTGC was calibrated using $(NH_4)_2SO_4$ (density = 1.77 g·cm^{-3}, and molar mass of 132 g·mol^{-1}) generated with the same experimental setup, and operating the DMA with a sheath:aerosol flow-rate ratio of 10:1; d for ammonium sulfate was then related to critical supersaturation by applying classical Köhler theory, using an effective van't Hoff factor of 2.5 [41,44]. The constant van't Hoff value is an approximation that can be improved with the use of the Pitzer Method. Multiple calibrations of the instrument were performed over the period of measurements, and each supersaturation was within 10% of the average.

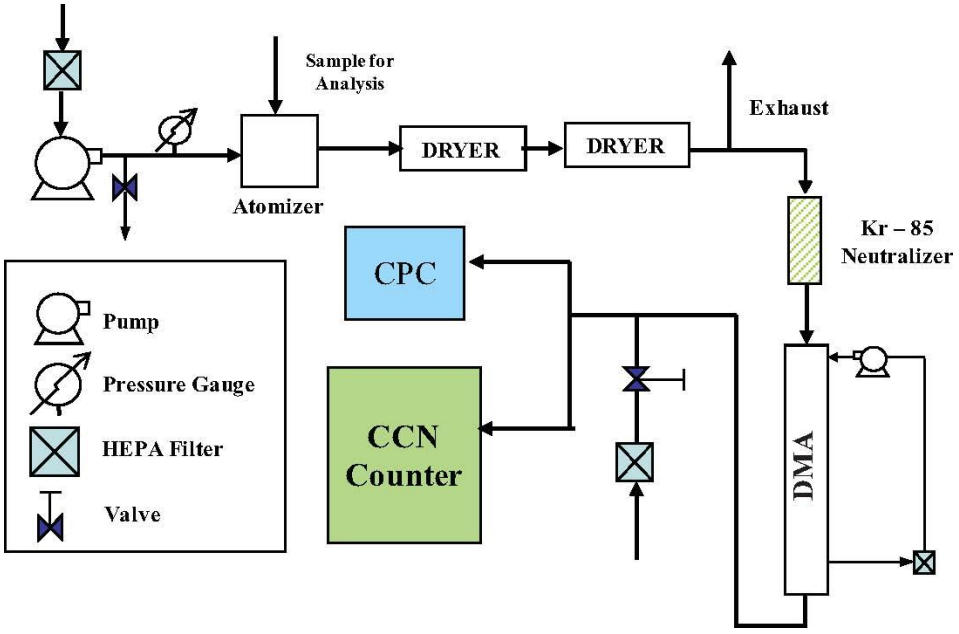

Figure 2. Experimental setup for characterizing size-resolved Cloud Condensation Nuclei activity of samples analyzed in this study.

2.3. Surface Tension Measurements

A CAM 200 pendant drop goniometer was used to measure bulk surface tension, σ, of the original samples and prescribed dilutions of them, following the approach of [33,35]. The instrument uses 5–6 mL of sample to form a drop at the end of a needle. The optical goniometer captures ~100 images of the droplet and computes droplet surface tension through application of the Young–Laplace equation; the standard deviations for $\sigma_{s/a}$ are <0.05 mN·m^{-1} for a given sample at one concentration. The measurements were then fit to the Szyskowski–Langmuir equation [45]:

$$\sigma = \sigma_w - \alpha T \ln(1 + \beta c) \quad (1)$$

where α, β are optimally fitted constants, T is temperature, σ_W is the surface tension of pure water and c is the dissolved carbon concentration (mg·C·L^{-1}). Each pendant drop was suspended 60 s before

surface tension was measured, in order to allow organics in the bulk to equilibrate with the droplet surface layer [46]. Table 1 provides a summary of the α and β parameters for all samples considered. Bulk measurements are known to not represent the droplet activation regime. Thus parameters derived from bulk measurements (Table 1) are applied to inferred droplet concentrations at activation [33–35,47].

2.4. Droplet Size Measurements of Activated CCN

The optical particle counter used for detection of CCN concentrations also provides the size of the activated droplets; thus the SMCA procedure can determine the size of activated CCN with known dry diameter at the exit of the CFSTGC. We adopt the method of Threshold Droplet Growth Analysis (TDGA) (e.g., but not limited to [39,48,49]) to detect the possible presence of droplets growing more slowly than calibration $(NH_4)_2SO_4$ aerosol [50]. If present then, a coupled measurement modeling approach can be used to infer the effective water vapor uptake coefficient [14,51]. TDGA compares the D_p of CCN with s_c equal to the instrument saturation (*i.e.*, CCN with a dry diameter equal to the cutoff diameter, d) against the wet diameter, $D_{p,(NH4)2SO4}$ of CCN with identical s_c, but composed of $(NH_4)_2SO_4$. If the presence of organics does not delay droplet growth, $D_p \sim D_{p,(NH4)2SO4}$ (e.g., [34,52]). Supersaturation depression is observed at high CCN concentration and can affect droplet size [53]. Thus both CCN measurement and analysis should account for CCN concentrations.

3. Analytical Theory

3.1. Köhler Theory

Köhler Theory Analysis (KTA) [33] can be used to infer the average molar volume (molecular weight, M_j, over density ρ_j) of the organic fraction, j, of CCN. It has been shown to work well for low molecular weight species, such as those presented here. Using measurements of s_C *versus* d to determine the Fitted CCN Activity parameter (FCA), $\omega = s_c d^{-1.5}$, KTA infers the average molar volume of the WSOC, $\frac{M_j}{\rho_j}$ [33,43],

$$\frac{M_j}{\rho_j} = \frac{\varepsilon_j \nu_j}{\frac{256}{27}\left(\frac{M_w}{\rho_w}\right)^2\left(\frac{1}{RT}\right)^3 \sigma^3 \omega^{-2} - \sum_{i \neq j} \frac{\rho_i}{M_i} \varepsilon_i \nu_i} \quad (2)$$

where M_w, ρ_w are the molecular weight and density of water, respectively, R is the universal gas constant, T is the ambient temperature, σ is the droplet surface tension at the point of activation, ε is the volume fraction, and ν is the effective van't Hoff factor. Subscripts I and j refer to the inorganic and organic components, respectively. ε_k is related to the mass fraction, m_k, of solute k (k being either of i or j) as:

$$\varepsilon_k = \frac{m_k/\rho_k}{\sum_{i \neq j} m_i/\rho_i + m_j/\rho_j} \quad (3)$$

Two measures of molar volume uncertainty are used: (*i*) the standard deviation of all the $\frac{M_j}{\rho_j}$ inferences (Equation (2)), and, (*ii*) estimates determined from, $\Delta\frac{M_j}{\rho_j} = \sqrt{\sum_x (\Phi_x \Delta x)^2}$, where Δx is the uncertainty of each of the measured parameters x, (*i.e.*, any of σ, ω, ε_i, ε_j, ν_i, and ν_j) and Φ_x is the

sensitivity of molar volume to x, $\Phi_x = \frac{\partial}{\partial x}(\frac{M_o}{\rho_o})$, using the formulas of [33,34,43]. The maximum of both estimates is the reported uncertainty of $\frac{M_j}{\rho_j}$. KTA has been shown to constrain molecular weight estimates for laboratory aerosol (having organic mass fraction between 20 and 50%) with an average error of 20% [33], 40% for complex biomass burning aerosol [43], 30% for secondary organic matter [35], and to within 25% for primary marine organic matter [34].

3.2. Inferring Surface Tension

The low concentration of WSOC in the PILS samples limits the determination (using direct measurements) of their surface tension depression for CCN-relevant concentrations. However, if CCN activity data are available for mixtures of WSOC and a salt (e.g., $(NH_4)_2SO_4$), KTA can be used to concurrently infer $\frac{M_j}{\rho_j}$ and σ using an iterative procedure [34]. If enough salt is present in the sample, the contribution of organic solute to s_c is small, and an iterative procedure is not required; the effect of the organic on CCN activity amounts to its impact on surface tension, and can then be inferred as [35],

$$\sigma = \sigma_w \left(\frac{S_c}{S_c^*}\right)^{2/3} \tag{4}$$

where s_c is the measured critical supersaturation, and s_c^* is the predicted value (from Köhler theory). Assuming $\sigma = \sigma_w$, the surface tension of pure water computed at the average CFSTGC column temperature [35], then

$$s_c^* = \frac{2}{3}\left(\frac{4M_w\sigma_w}{RT\rho_w}\right)^{3/2}\left(\frac{M_w d^3}{\rho_w}\sum_i \frac{\varepsilon_i \nu_i \rho_i}{M_i}\right)^{-1/2} \tag{5}$$

where "i" denotes all inorganic solutes present in the aerosol. Each surface tension inference is then related to the WSOC concentration at the critical diameter (Equation (6) of [34], and fit to the Szyskowski–Langmuir adsorption isotherm (Equation (1)). The partitioning of the surfactant from the bulk to the droplet monolayer should be considered. This method of inferring surface tension depression has been shown to work well for dissolved organic matter isolated from seawater [34]. Thus in the case of marine POMA, where the surfactant may partition mostly to the surface, partitioning effects are less important than bulk properties and why Moore *et al.* [34] were able to achieve good closure.

4. Results and Discussion

4.1. Surface Tension

For the low WSOC concentrations measured in the PILS samples, organics have minimal effect on surface tension (Figure 3). Hence, Equation (4) is used to infer σ at carbon concentrations relevant for CCN activation (roughly 1000 mg·C·L^{-1}). WSOC from biomass burning aerosol and marine aerosol have been shown to contain strong surfactants that depress surface tension by 25%–42% [43,47,54,55] at similar concentration. The inferred σ values for both SC and CR aerosol (Figure 3) exhibit weak surface tension depression ($-\Delta\sigma/\sigma \simeq 5\%$) at concentrations >1000 mg·C·L^{-1}. The surface tension

depression results are similar to results from dissolved organic marine matter [34]. Both CR and SC samples were influenced by ship emissions, SOMA, and POMA and contained soluble organics. The solubility of the organics is unknown, however the potential effects of limited solubility on CCN activity for SC samples may be outweighed by significant depression in surface tension at the droplet surface (Figure 3). Finding the average organic molar mass from KTA will help constrain if the SC and CR samples indeed have different organic aerosol compositions that affect aerosol solubility and surfactant properties.

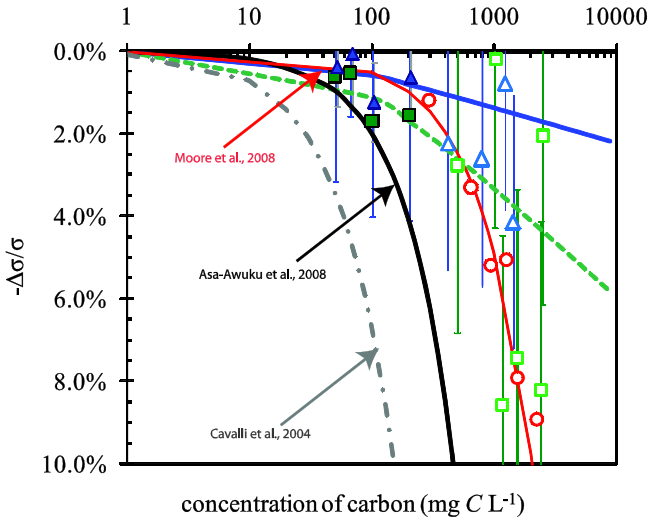

Figure 3. Surface tension depression as a function of dissolved carbon concentration. Measurements (closed symbols) and Inferred values (open symbols) of the CR (blue triangles) and SC aerosol (green squares) are shown as data points. For comparison, curves are added with data from freshly emitted biomass burning aerosol (solid black; [43], marine organic aerosol (grey dash-dot; [54]) and dissolved marine organic matter (solid red; [34]).

4.2. CCN Activity

Figures 4 and 5 show the critical supersaturation, s_c, as a function of dry diameter, d, for aerosol atomized from both CR and SC samples. The data for $(NH_4)_2SO_4$ aerosol have been added for comparison. Data for $(NH_4)_2SO_4$ are consistent with the expectation that the aerosol is highly CCN active, lies to the left of both CR and SC data sets, and behaves as classical Kohler CCN without surface tension depression. The activation slope of particles composed of soluble and insoluble material should exhibit a s_c that scales with $d^{-1.5}$ (e.g., $(NH_4)_2SO_4$ data in Figure 4). At low supersaturations ($s_c \leq 0.6\%$), the WSOC concentration at the point of activation was low (<1000 mg·C·L^{-1}) and surface tension depression was small (Figure 3), hence $s_c \sim d^{-1.5}$ for both samples, and KTA is applied for this region of the CCN spectrum. The CR sample contained material that was less hygroscopic than sulfate, but more hygroscopic than in the SC sample (*i.e.*, for a given s, the d of the CR is greater than SC, Figure 4). SC and CR activation curves converge at high s, likely because the WSOC concentration is high enough to notably decrease surface depression, more for organics in SC than for CR (Figure 3). The difference in CCN activity is consistent with studies to date (e.g., [16,56]), showing that hygroscopic components tend to be incorporated in cloud droplets where their less hygroscopic counterparts prefer to remain in the interstitial air. It is also noted that the CR

samples excluded droplets <5 μm diameter thus the excluded smaller droplets may potentially contain less hygroscopic materials.

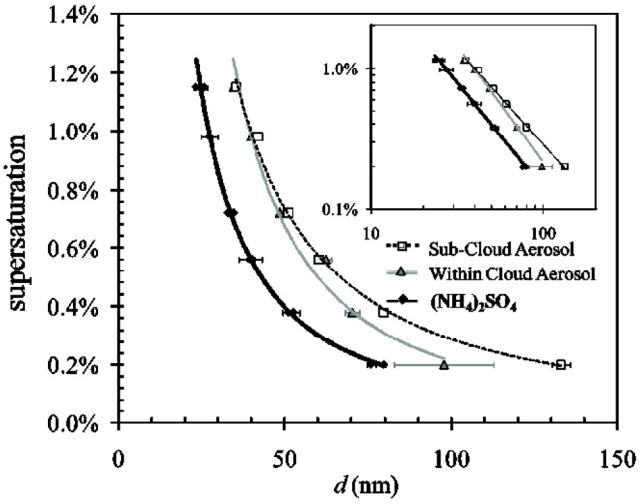

Figure 4. CCN activity of SC and CR samples. $(NH_4)_2SO_4$ (solid black line) is added for comparison. The CCN activity curve exponents for $(NH_4)_2SO_4$, CR, and SC are −1.51, −1.66, and −1.35, respectively.

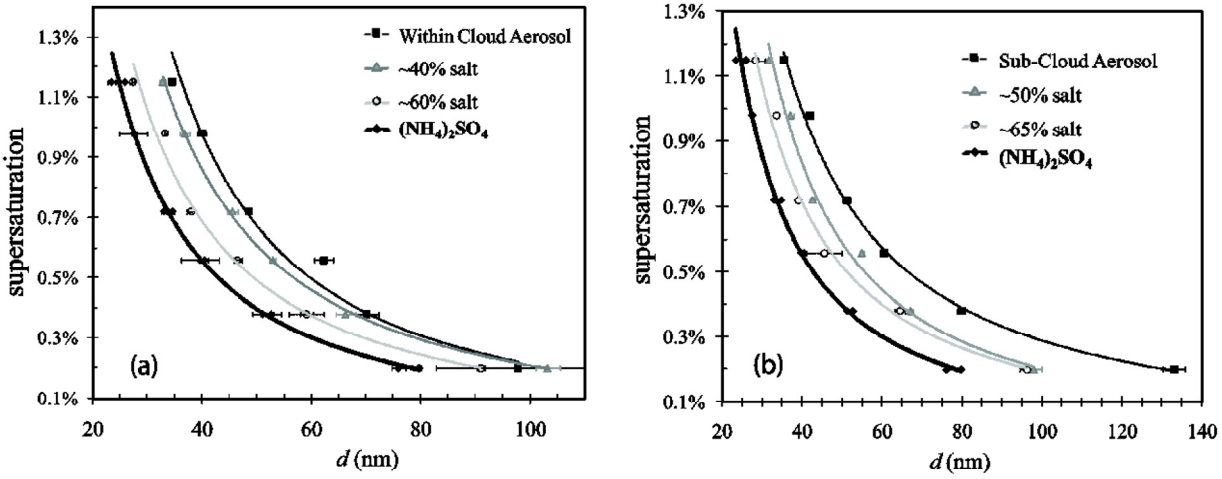

Figure 5. CCN activity of MASE samples with the addition of $(NH_4)_2SO_4$. Salt contents are expressed in terms of mass fraction. (**a**) Cloud Residuals and (**b**) Sub-Cloud samples.

4.3. Inferred Molar Volumes and Uncertainties

Application of KTA requires the input of the organic mass concentration, $m_{organic}$, which is obtained by dividing the WSOC carbon concentration (Table 1) by the carbon-to-organic mass ratio, *C/OC*. In this study, $C/OC \approx 0.27$ is applied, the value for oxalic acid ($C_2H_6O_4$, 90 g·moL^{-1}), the most abundant organic acid measured in our samples (Table 1). $C/OC \approx 0.27$ is very close to 0.29, the value for dissolved primary organic marine matter and marine coarse mode aerosol [34,54]. Here we expect it to apply to the whole sample. The van't Hoff factor for the organic fraction is assumed to be unity. The presence of organics from ship emissions are assumed to introduce little variability to the organic mass fractions estimated. The ionic composition taken from the chemical analysis of the PILS vials is

then converted into a mixture of inorganic salts and organics with the ISORROPIA II aerosol thermodynamic equilibrium model [57]. Lu *et al.* [36] find the composition of aerosol sampled to be bimodal, composed of ammonium bisulfate and sea-salt; when samples are mixed in the PILS, chloride depletion is both expected and observed in the samples (Table 2). The results of the KTA analysis for each sample are summarized in Tables 3 and 4. Assuming an organic density of 1.4 $g \cdot cm^{-3}$ [35,58], the SC sample has a high inferred molecular weight (M_j = 2413 ± 536 $g \cdot mol^{-1}$; Table 4), possibly long-chained aliphatic compounds within primary organic matter transferred to the aerosol from bubble bursting at the seawater surface [16,34,54,59,60]. The marine nature of the SC sample is further supported by its inferred surface tension depression (Figure 3, which is remarkably consistent with dissolved organic matter [34]. The average molecular weight inferred for CR aerosol is substantially less (143 ± 25 $g \cdot mol^{-1}$; Table 3), consistent with the presence of low molecular weight carboxylic acids (*i.e.*, C_2–C_9 mono and dicarboxylic acids) measured in cloud-processed marine aerosol [15]. Water-soluble oxidation products from ship VOC emissions can also contribute to the WSOC, although the information at hand is not sufficient to conclusively show this. As in previous KTA studies (e.g., [33]), inferred average molar volume is subject to an estimated 30% error; the greatest source of uncertainty stems from the FCA parameter (Tables 3 and 4). The low depression in surface tension (Figure 3) suggests that the molecular weight distribution in the WSOC may not contain compounds characteristic of HULIS (300–750 $g \cdot mol^{-1}$) [43,47], but instead can be described by the superposition of two "modes", one from SOMA (low molecular weight compounds), and one from POMA (higher molecular weight compounds). For the SC sample, we assume that the SOMA is primarily composed of oxalic acid (90 $g \cdot mol^{-1}$, the predominant compound identified in the PILS samples and constitutes 0.6% of the organic mass, Table 1), and the remaining mass (99.4%) is POMA characteristic of Redfield-type molecules, $(CHO_2)_{106}(NH_3)_{16}H_3PO_4$, 3444 $g \cdot mol^{-1}$ [61,62]. With this assumed two-component model composition, the average M_j in SC is equal to 2852 $g \cdot mol^{-1}$, and consistent (to within uncertainty) with the inferred KTA value (Table 4). Similarly, if most of the organic in the CR aerosol is a mixture of ship emissions and oxalate, and that the POMA mode is consistent with phenathrene (178 $g \cdot mol^{-1}$and 99.6% of the organic mass), and SOMA with oxalic acid (90 $g \cdot mol^{-1}$ and 0.4% of the organic mass, Table 1), the average molar mass for the organic distribution yields 177 $g \cdot mol^{-1}$, a value within 25% of our KTA estimate.

Table 2. Mass fraction (%) of constituents in the aerosol samples considered in this study. Composition of the inorganic fraction was obtained by an aerosol thermodynamic equilibrium model (ISORROPIA-II), using the ionic composition of Table 1.

	Cloud Residuals (CR)	**Sub-Cloud (SC)**
Organic	88.3	82
NH_4	3.4	3.6
NaCl	0.6	0
$(NH_4)_2SO_4$	0.0	5.1
$NaNO_3$	2.3	0.0
NH_4NO_3	0.0	2.4
Na_2SO_4	4.1	7.0
$CaSO_4$	1.1	0.0

Table 3. Köhler Theory Analysis for Cloud-Residual (CR) samples.

Property x *(units)*	Average Value of x	Uncertainty Δx	Sensitivity, Φ_x ($m^3 \cdot mol^{-1} \cdot x^{-1}$)	$\frac{M_j}{\rho_j}$ Contribution (%)
σ ($N \cdot m^{-1}$)	6.89×10^{-2}	1.38×10^{-3}	3.83×10^{-3}	5.72
ω ($m^{1.5}$)	6.80×10^{-2}	5.53×10^{-15}	2.59×10^{9}	12.42
ν_{NH_4Cl}	2	0.5	6.43×10^{-6}	3.49
ν_{NaCl}	2	0.5	1.54×10^{-6}	0.83
ν_{NaNO_3}	2	0.5	4.18×10^{-6}	2.27
$\nu_{Na_2SO_4}$	3	-	-	-
$\nu_{organic}$	1	0.20	4.39×10^{-5}	9.52
ε_{NaNO_3}	0.05	-	-	-
$\varepsilon_{Na_2SO_4}$	0.07	-	-	-
ε_{NH_4Cl}	0.10	1.95×10^{-3}	8.50×10^{-4}	0.80
$\varepsilon_{organic}$	0.88	6.36×10^{-3}	4.10×10^{-3}	2.82
ρ_{NH_4Cl}	1.53	-	-	-
ρ_{NaCl}	2.16	-	-	-
ρ_{NaNO_3}	2.3	-	-	-
$\rho_{Na_2SO_4}$	2.68	-	-	-
$\rho_{organic}$	1.4	-	-	-
$\rho_{aerosol}$	1.59	-	-	-
M_J/ρ_J ($cm^3 \cdot mol^{-1}$)	1.60×10^{-4}	17.5%	-	-
M_J ($g \cdot mol^{-1}$)	143	25	-	-

Table 4. Köhler Theory Analysis for Sub-Cloud (SC) samples.

Property x *(units)*	Average Value of x	Uncertainty Δx	Sensitivity, Φ_x ($m^3 \cdot mol^{-1} \cdot x^{-1}$)	$\frac{M_j}{\rho_j}$ Contribution (%)
σ ($N \cdot m^{-1}$)	6.58×10^{-2}	1.32×10^{-3}	1.97×10^{-3}	8.37
ω ($m^{1.5}$)	8.75×10^{-14}	4.43×10^{-15}	9.89×10^{9}	14.13
ν_{NH_4Cl}	2	0.5	6.35×10^{-5}	10.24
$\nu_{(NH_4)_2SO_4}$	2.5	0.5	3.74×10^{-6}	0.60
$\nu_{NH_4NO_3}$	2	0.5	2.82×10^{-6}	0.45
$\nu_{Na_2SO_4}$	3	-	-	-
$\nu_{organic}$	1	0.20	7.21×10^{-5}	4.65
$\varepsilon_{NH_4NO_3}$	0.06	-	-	-
$\varepsilon_{Na_2SO_4}$	0.10	-	-	-
ε_{NH_4Cl}	0.09	1.95×10^{-3}	4.21×10^{-3}	2.64
$\varepsilon_{(NH_4)_2SO_4}$	0.12	2.03×10^{-3}	4.10×10^{-3}	2.69
$\varepsilon_{organic}$	0.82	6.36×10^{-3}	4.63×10^{-3}	9.50
ρ_{NH_4Cl}	1.53	-	-	-
$\rho_{(NH_4)_2SO_4}$	1.77	-	-	-
$\rho_{NH_4NO_3}$	1.73	-	-	-
$\rho_{Na_2SO_4}$	2.68	-	-	-
M_J/ρ_J ($cm^3 \cdot mol^{-1}$)	1.72×10^{-3}	22.2%	-	-
M_J ($g \cdot mol^{-1}$)	2413	536	-	-

4.4. The Effect of Organics on Droplet Growth Kinetics

Figure 6 illustrates the OPC droplet size measurements for all supersaturations and samples considered. The flow rate within the instrument was maintained at 0.5 L·min^{-1} and the sheath to aerosol flow rate ratio was 10:1 to so that particles have the same residence time in the CFSTGC. Similar to the WSOC droplet data presented in [34,35,52,63], almost all of the growth droplet data lie within the measurement uncertainty and are in agreement with $(NH_4)_2SO_4$ calibration aerosol. According to TDGA, the water uptake coefficient is similar to that of the water uptake coefficient of $(NH_4)_2SO_4$ ($\alpha_c \sim \alpha_{(NH4)2SO4}$). Given that the water uptake coefficient, $\alpha_{(NH4)2SO4} \sim 0.2$ [50,51], this suggest that the WSOC would not slow down activation kinetics of CCN compared to $(NH_4)_2SO_4$. This is consistent with the analysis of CCN data collected from a wide range of environments [51]. The WSOC does not appreciably impact droplet growth kinetics (or the effective water vapor mass transfer coefficient) as aerosol particles produced from the SC and CR grow like $(NH4)_2SO_4$.

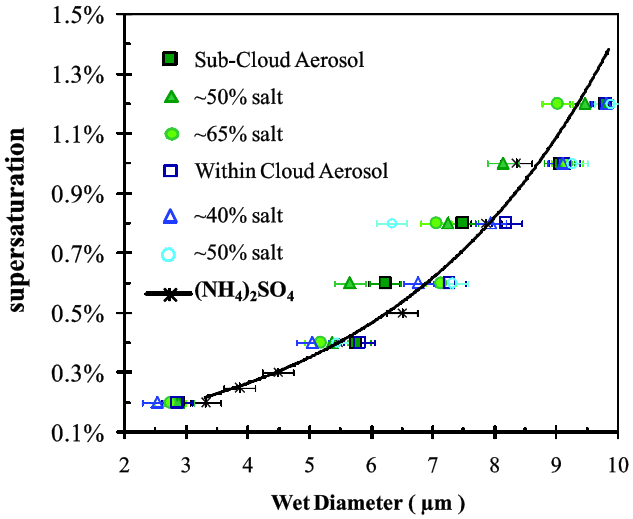

Figure 6. Size of activated CCN generated from the cloud residual samples (CR, solid symbols), sub-cloud samples (SC, open symbols) and $(NH_4)_2SO_4$ (solid black line). Droplet sizes are presented for CCN with s_c equal to the instrument supersaturation.

5. Summary and Implications

CCN activity, chemical composition and droplet growth measurements coupled with Köhler Theory Analysis are used to characterize the cloud droplet formation potential of water-soluble organic matter collected from cloud droplet (CR) residuals and sub-cloud (SC) aerosol during the MASE 2005 campaign over the eastern Pacific Ocean off the coast of California. The organics within CR samples were found to be more hygroscopic than in the SC sample, most likely from the enhanced levels of soluble organic acids (e.g., oxalic) formed during cloud processing. Both the direct and inferred surface tension measurements show neither sample contained strong surfactants; in fact, surface tension depression is consistent with the effect from primary marine organic matter.

Inferred average molecular weights of both CR and SC samples are consistent with a bimodal molecular weight distribution; one composed of oxalic acid (produced through glyoxylic oxidation or the oxidative decay of larger diacids in cloud droplets [15]) with primary organic matter (SC sample),

or, organics from ship emissions (CR sample). These results are consistent with recently published work [18,64] that shows SOMA as a significant contributor to CCN activity in marine regions. Finally, all samples display similar droplet growth kinetics to CCN composed of $(NH_4)_2SO_4$, suggesting that water-soluble organics do not significantly impact the growth rate of CCN. Hence, CCN activity of the organics affects CCN activity through their contribution of solute from SOMA and possibly a slight surface tension depression from POMA. In both cases, increasing the size of CCN will also have a major impact, which is not shown here.

Acknowledgments

The work in this study was supported by an NSF CAREER Award. In addition, we would like to thank Dr. Rodney Weber and his students at the Georgia Institute of Technology for the use of the Total Organic Carbon (TOC) Turbo Siever Analyzer and Dr. Christos Fountoukis for his help in running the ISORROPIA II code.

Author Contributions

Akua Asa-Awuku is co-corresponding author and conducted laboratory experiments, collected and analyzed data sets, and played a significant role in the writing of the manuscript. Armin Sorooshian collected samples in the field, aided in analysis and writing. Richard C. Flagan and John H. Seinfeld devised flight experiments. Athanasios Nenes is co-corresponding author and conceived and devised experiments, analysis, and significantly contributed to writing.

Conflicts of Interest

The authors declare no conflict of interest.

References

1. Saxena, P.; Hildemann, L.M.; McMurry, P.H.; Seinfeld, J.H. Organics alter hygroscopic behavior of atmospheric particles. *J. Geophys. Res.* **1995**, *100*, 18755–18770.
2. Facchini, M.C.; Fuzzi, S.; Zappoli, S.; Andracchio, A.; Gelencsér, A.; Kiss, G.; Krivácsy, Z.; Mészáros, E.; Hansson, H.-C.; Alsberg, T.; *et al.* Partitioning of the organic aerosol component between fog droplets and interstitial air. *J. Geophys. Res.* **1999**, *104*, 26821–26832.
3. Nenes, A.; Charlson, R.J.; Facchini, M.C.; Kulmala, M.; Laaksonen, A.; Seinfeld, J.H. Can chemical effects on cloud droplet number rival the first indirect effect? *Geophys. Res. Lett.* **2002**, *29*, 29–21.
4. Decesari, S.; Facchini, M.C.; Mircea, M.; Cavalli, F.; Fuzzi, S. Solubility properties of surfactants in atmospheric aerosol and cloud/fog water samples. *J. Geophys. Res.* **2003**, *108,* 1984–2012.
5. Ervens, B.; Feingold, G.; Clegg, S.L.; Kreidenweis, S.M. A modeling study of aqueous production of dicarboxylic acids: 2. Implications for cloud microphysics. *J. Geophys. Res.* **2004**, *109*, D15206.

6. Saxena, P.; Hildemann, L.M. Water-soluble organics in atmospheric particles: A critical review of the literature and application of thermodynamics to identify candidate compounds. *J. Atmos. Chem.* **1996**, *24*, 57–109.
7. Mircea, M.; Facchini, M.C.; Decesari, S.; Fuzzi, S.; Charlson, R.J. The influence of the organic aerosol component on CCN supersaturation spectra for different aerosol types. *Tellus. B Chem. Phys. Meteorol.* **2002**, *54*, 74–81.
8. Alfonso, L.; Raga, G.B. The influence of organic compounds on the development of precipitation acidity in maritime clouds. *Atmos. Chem. Phys.* **2004**, *4*, 1097–1111.
9. O'Dowd, C.D.; Facchini, M.C.; Cavalli, F.; Ceburnis, D.; Mircea, M.; Decesari, S.; Fuzzi, S.; Yoon, Y.J.; Putaud, J.-P. Biogenically driven organic contribution to marine aerosol. *Nature* **2004**, *431*, 676–680.
10. Zhao, C.; Ishizaka, Y.; Peng, D. Numerical Study on Impacts of Multi-Component Aerosols on Marine Cloud Microphysical Properties. *J. Meteorol. Soc. Jpn. Ser. II* **2005**, *83*, 977–986.
11. Kanakidou, M.; Seinfeld, J.H.; Pandis, S.N.; Barnes, I.; Dentener, F.J.; Facchini, M.C.; Van Dingenen, R.; Ervens, B.; Nenes, A.; Nielsen, C.J.; *et al.* Organic aerosol and global climate modelling: A review. *Atmos. Chem. Phys.* **2005**, *5*, 1053–1123.
12. Yoon, Y.J.; Ceburnis, D.; Cavalli, F.; Jourdan, O.; Putaud, J.P.; Facchini, M.C.; Decesari, S.; Fuzzi, S.; Sellegri, K.; Jennings, S.G.; *et al.* Seasonal characteristics of the physicochemical properties of North Atlantic marine atmospheric aerosols. *J. Geophys. Res.* **2007**, *112*, D04206.
13. Ovadnevaite, J.; Ceburnis, D.; Martucci, G.; Bialek, J.; Monahan, C.; Rinaldi, M.; Facchini, M.C.; Berresheim, H.; Worsnop, D.R.; O'Dowd, C. Primary marine organic aerosol: A dichotomy of low hygroscopicity and high CCN activity. *Geophys. Res. Lett.* **2011**, *38*, L21806.
14. Moore, R.H.; Raatikainen, T.; Langridge, J.M.; Bahreini, R.; Brock, C.A.; Holloway, J.S.; Lack, D.A.; Middlebrook, A.M.; Perring, A.E.; Schwarz, J.P.; *et al.* CCN spectra, hygroscopicity, and droplet activation kinetics of secondary organic aerosol resulting from the 2010 Deepwater Horizon oil spill. *Environ. Sci. Technol.* **2012**, *46*, 3093–3100.
15. Sorooshian, A.; Lu, M.-L.; Brechtel, F.J.; Jonsson, H.; Feingold, G.; Flagan, R.C.; Seinfeld, J.H. On the source of organic acid aerosol layers above clouds. *Environ. Sci. Technol.* **2007**, *41*, 4647–4654.
16. Ceburnis, D.; O'Dowd, C.D.; Jennings, G.S.; Facchini, M.C.; Emblico, L.; Decesari, S.; Fuzzi, S.; Sakalys, J. Marine aerosol chemistry gradients: Elucidating primary and secondary processes and fluxes. *Geophys. Res. Lett.* **2008**, *35*, L07804.
17. Rinaldi, M.; Decesari, S.; Finessi, E.; Giulianelli, L.; Carbone, C.; Fuzzi, S.; O'Dowd, C.D.; Ceburnis, D.; Facchini, M.C. Primary and secondary organic marine aerosol and oceanic biological activity: Recent results and new perspectives for future studies. *Adv. Meteorol.* **2010**, *2010*, 1–10.
18. Coggon, M.M.; Sorooshian, A.; Wang, Z.; Metcalf, A.R.; Frossard, A.A.; Lin, J.J.; Craven, J.S.; Nenes, A.; Jonsson, H.H.; Russell, L.M.; *et al.* Ship impacts on the marine atmosphere: Insights into the contribution of shipping emissions to the properties of marine aerosol and clouds. *Atmos. Chem. Phys.* **2012**, *12*, 8439–8458.

19. Sorooshian, A.; Wang, Z.; Coggon, M.M.; Jonsson, H.H.; Ervens, B. Observations of sharp oxalate reductions in stratocumulus clouds at variable altitudes: Organic acid and metal measurements during the 2011 E-PEACE campaign. *Environ. Sci. Technol.* **2013**, *47*, 7747–7756.
20. Sorooshian, A.; Varutbangkul, V.; Brechtel, F.J.; Ervens, B.; Feingold, G.; Bahreini, R.; Murphy, S.M.; Holloway, J.S.; Atlas, E.L.; Buzorius, G.; *et al.* Oxalic acid in clear and cloudy atmospheres: Analysis of data from International Consortium for Atmospheric Research on Transport and Transformation 2004. *J. Geophys. Res. D: Atmos.* **2006**, *111*, D10S27.
21. Ervens, B.; Feingold, G.; Frost, G.J.; Kreidenweis, S.M. A modeling study of aqueous production of dicarboxylic acids: 1. Chemical pathways and speciated organic mass production. *J. Geophys. Res.* **2004**, *109*, D15205.
22. Lim, H.; Carlton, A.G.; Turpin, B.J. Isoprene forms secondary organic aerosol in Atlanta: Results from time-resolved measurements during the Atlanta supersite experiment. *Environ. Sci. Technol.* **2005**, *39*, 4441–4446.
23. Carlton, A.G.; Turpin, B.J.; Lim, H.-J.; Altieri, K.E.; Seitzinger, S. Link between isoprene and secondary organic aerosol (SOA): Pyruvic acid oxidation yields low volatility organic acids in clouds. *Geophys. Res. Lett.* **2006**, *33*, L06822.
24. Coggon, M.M.; Sorooshian, A.; Wang, Z.; Craven, J.S.; Metcalf, A.R.; Lin, J.J.; Nenes, A.; Jonsson, H.H.; Flagan, R.C.; Seinfeld, J.H. Observations of continental biogenic impacts on marine aerosol and clouds off the coast of California. *J. Geophys. Res. D: Atmos.* **2014**, *119*, 6724–6748.
25. Eyring, V.; Köhler, H.W.; van Aardenne, J.; Lauer, A. Emissions from international shipping: 1. The last 50 years. *J. Geophys. Res.* **2005**, *110*, D17305.
26. Zheng, Z.; Tang, X.; Asa-Awuku, A.; Jung, H.S. Characterization of a method for aerosol generation from heavy fuel oil (HFO) as an alternative to emissions from ship diesel engines. *J. Aerosol Sci.* **2010**, *41*, 1143–1151.
27. Russell, L.M.; Noone, K.J.; Ferek, R.J.; Pockalny, R.A.; Flagan, R.C.; Seinfeld, J.H. Combustion Organic Aerosol as Cloud Condensation Nuclei in Ship Tracks. *J. Atmos. Sci.* **2000**, *57*, 2591–2606.
28. Twomey, S. Pollution and the planetary albedo. *Atmos. Environ.* **1974**, *8*, 1251–1256.
29. Coakley, J.A.; Bernstein, R.L.; Durkee, P.A. Effect of ship-stack effluents on cloud reflectivity. *Science* **1987**, *237*, 1020–1022.
30. Albrecht, B.A. Aerosols, cloud microphysics, and fractional cloudiness. *Science* **1989**, *245*, 1227–1230.
31. Ackerman, A.S.; Toon, O.B.; Taylor, J.P.; Johnson, D.W.; Hobbs, P.V.; Ferek, R.J. Effects of aerosols on cloud albedo: Evaluation of Twomey's parameterization of cloud susceptibility using measurements of ship tracks. *J. Atmos. Sci.* **2000**, *57*, 2684–2695.
32. Moore, R.H.; Cerully, K.; Bahreini, R.; Brock, C.A.; Middlebrook, A.M.; Nenes, A. Hygroscopicity and composition of California CCN during summer 2010. *J. Geophys. Res.* **2012**, *117*, D00V12
33. Padró, L.T.; Asa-Awuku, A.; Morrison, R.; Nenes, A. Inferring thermodynamic properties from CCN activation experiments: Single-component and binary aerosols. *Atmos. Chem. Phys.* **2007**, *7*, 5263–5274.

34. Moore, R.H.; Ingall, E.D.; Sorooshian, A.; Nenes, A. Molar mass, surface tension, and droplet growth kinetics of marine organics from measurements of CCN activity. *Geophys. Res. Lett.* **2008**, *35*, L07801.
35. Asa-Awuku, A.; Nenes, A.; Gao, S.; Flagan, R.C.; Seinfeld, J.H. Water-soluble SOA from Alkene ozonolysis: Composition and droplet activation kinetics inferences from analysis of CCN activity. *Atmos. Chem. Phys.* **2010**, *10*, 1585–1597.
36. Lu, M.-L.; Conant, W.C.; Jonsson, H.H.; Varutbangkul, V.; Flagan, R.C.; Seinfeld, J.H. The Marine Stratus/Stratocumulus Experiment (MASE): Aerosol-cloud relationships in marine stratocumulus. *J. Geophys. Res. D: Atmos.* **2007**, *112*, D10209.
37. Marple, V.A.; Chien, C.M. Virtual impactors: A theoretical study. *Environ. Sci. Technol.* **1980**, *14*, 976–985.
38. Noone, K.J.; Ogren, J.A.; Heintzenberg, J.; Charlson, R.J.; Covert, D.S. Design and calibration of a counterflow virtual impactor for sampling of atmospheric fog and cloud droplets. *Aerosol Sci. Technol.* **1988**, *8*, 235–244.
39. Roberts, G.C.; Nenes, A. A continuous-flow streamwise thermal-gradient CCN chamber for atmospheric measurements. *Aerosol Sci. Technol.* **2005**, *39*, 206–221.
40. Lance, S.; Nenes, A.; Medina, J.; Smith, J.N. Mapping the operation of the DMT continuous flow CCN counter. *Aerosol Sci. Technol.* **2006**, *40*, 242–254.
41. Rose, D.; Gunthe, S.S.; Mikhailov, E.; Frank, G.P.; Dusek, U.; Andreae, M.O.; Pöschl, U. Calibration and measurement uncertainties of a continuous-flow cloud condensation nuclei counter (DMT-CCNC): CCN activation of ammonium sulfate and sodium chloride aerosol particles in theory and experiment. *Atmos. Chem. Phys.* **2008**, *8*, 1153–1179.
42. Moore, R.H.; Nenes, A.; Medina, J. Scanning mobility CCN analysis—A method for fast measurements of size-resolved CCN distributions and activation kinetics. *Aerosol Sci. Technol.* **2010**, *44*, 861–871.
43. Asa-Awuku, A.; Sullivan, A.P.; Hennigan, C.J.; Weber, R.J.; Nenes, A. Investigation of molar volume and surfactant characteristics of water-soluble organic compounds in biomass burning aerosol. *Atmos. Chem. Phys.* **2008**, *8*, 799–812.
44. Brechtel, F.J.; Kreidenweis, S.M. Predicting particle critical supersaturation from hygroscopic growth measurements in the humidified TDMA. Part I: Theory and sensitivity studies. *J. Atmos. Sci.* **2000**, *57*, 1854–1871.
45. Langmuir, I. The constitution and fundamental properties of solids and liquids. II. liquids.1. *J. Am. Chem. Soc.* **1917**, *39*, 1848–1906.
46. Taraniuk, I.; Graber, E.R.; Kostinski, A.; Rudich, Y. Surfactant properties of atmospheric and model humic-like substances (HULIS). *Geophys. Res. Lett.* **2007**, *34*, L16807
47. Giordano, M.R.; Short, D.Z.; Hosseini, S.; Lichtenberg, W.; Asa-Awuku, A.A. Changes in droplet surface tension affect the observed hygroscopicity of photochemically aged biomass burning aerosol. *Environ. Sci. Technol.* **2013**, *47*, 10980–10986.
48. Lance, S.; Nenes, A.; Mazzoleni, C.; Dubey, M.K.; Gates, H.; Varutbangkul, V.; Rissman, T.A.; Murphy, S.M.; Sorooshian, A.; Flagan, R.C.; *et al.* Cloud condensation nuclei activity, closure, and droplet growth kinetics of Houston aerosol during the Gulf of Mexico Atmospheric Composition and Climate Study (GoMACCS). *J. Geophys. Res. D: Atmos.* **2009**, *114*, D00F15.

49. Asa-Awuku, A.; Moore, R.H.; Nenes, A.; Bahreini, R.; Holloway, J.S.; Brock, C.A.; Middlebrook, A.M.; Ryerson, T.B.; Jimenez, J.L.; DeCarlo, P.F.; *et al.* Airborne cloud condensation nuclei measurements during the 2006 Texas Air Quality Study. *J. Geophys. Res. D: Atmos.* **2011**, *116*, D11201.
50. Raatikainen, T.; Moore, R.H.; Lathem, T.L.; Nenes, A. A coupled observation—modeling approach for studying activation kinetics from measurements of CCN activity. *Atmos. Chem. Phys.* **2012**, *12*, 4227–4243.
51. Raatikainen, T.; Nenes, A.; Seinfeld, J.H.; Morales, R.; Moore, R.H.; Lathem, T.L.; Lance, S.; Padró, L.T.; Lin, J.J.; Cerully, K.M.; *et al.* Worldwide data sets constrain the water vapor uptake coefficient in cloud formation. *Proc. Natl. Acad. Sci. USA* **2013**, *110*, 3760–3764.
52. Engelhart, G.J.; Asa-Awuku, A.; Nenes, A.; Pandis, S.N. CCN activity and droplet growth kinetics of fresh and aged monoterpene secondary organic aerosol. *Atmos. Chem. Phys.* **2008**, *8*, 3937–3949.
53. Lathem, T.L.; Nenes, A. Water vapor depletion in the DMT continuous-flow CCN chamber: Effects on supersaturation and droplet growth. *Aerosol Sci. Technol.* **2011**, *45*, 604–615.
54. Cavalli, F.; Facchini, M.C.; Decesari, S.; Mircea, M.; Emblico, L.; Fuzzi, S.; Ceburnis, D.; Yoon, Y.J.; O'Dowd, C.D.; Putaud, J.-P.; *et al.* Advances in characterization of size-resolved organic matter in marine aerosol over the North Atlantic. *J. Geophys. Res. D: Atmos.* **2004**, *109*, D24215.
55. Kiss, G.; Tombácz, E.; Hansson, H.-C. Surface tension effects of humic-like substances in the aqueous extract of tropospheric fine aerosol. *J. Atmos. Chem.* **2005**, *50*, 279–294.
56. Hallberg, A.; Ogren, J.A.; Noone, K.J.; Okada, K.; Heintzenberg, J.; Svenningsson, I.B. The Influence of Aerosol Particle Composition on Cloud Droplet Formation. In *The Kleiner Feldberg Cloud Experiment 1990*; Springer Netherlands: Houten, the Netherlands, 1994; pp. 153–171.
57. Fountoukis, C.; Nenes, A. ISORROPIA II: A computationally efficient thermodynamic equilibrium model for K^+-Ca^{2+}-Mg^{2+}-NH^{4+}-Na^+-SO_4^{2-}-NO_3^--Cl^--H_2O aerosols. *Atmos. Chem. Phys.* **2007**, *7*, 4639–4659.
58. Turpin, B.J.; Lim, H.-J. Species contributions to $PM_{2.5}$ mass concentrations: Revisiting common assumptions for estimating organic MASS. *Aerosol Sci. Technol.* **2001**, *35*, 602–610.
59. Oppo, C.; Bellandi, S.; Degli Innocenti, N.; Stortini, A.M.; Loglio, G.; Schiavuta, E.; Cini, R. Surfactant components of marine organic matter as agents for biogeochemical fractionation and pollutant transport via marine aerosols. *Mar. Chem.* **1999**, *63*, 235–253.
60. Hansell, D.A.; Carlson, C.A. *Biogeochemistry of Marine Dissolved Organic Matter*; Academic Press: London, UK, 2002.
61. Redfield, A.C.; Ketchum, B.H.; Richards, F.A. The influence of organisms on the composition of sea-water. *Sea* **1963**, *2*, 26–77.
62. Schulz, H.D.; Zabel, M. *Marine Geochemistry*; Springer Science & Business Media: Berlin, Germany, 2013.
63. Asa-Awuku, A.; Engelhart, G.J.; Lee, B.H.; Pandis, S.N.; Nenes, A. Relating CCN activity, volatility, and droplet growth kinetics of β-caryophyllene secondary organic aerosol. *Atmos. Chem. Phys. Disc.* **2008**, *8*, 10105–10151.

64. Wonaschütz, A.; Coggon, M.; Sorooshian, A.; Modini, R.; Frossard, A.A.; Ahlm, L.; Mülmenstädt, J.; Roberts, G.C.; Russell, L.M.; Dey, S.; *et al.* Hygroscopic properties of smoke-generated organic aerosol particles emitted in the marine atmosphere. *Atmos. Chem. Phys.* **2013**, *13*, 9819–9835.